

The random field Ising model with an asymmetric and anisotropic trimodal probability distribution

Ioannis A. Hadjiagapiou *

*Section of Solid State Physics, Department of Physics, University of Athens,
Panepistimiopolis, GR 15784 Zografos, Athens, Greece*

Abstract

The Ising model in the presence of a random field, drawn from the asymmetric and anisotropic trimodal probability distribution $P(h_i) = p \delta(h_i - h_0) + q \delta(h_i + \lambda * h_0) + r \delta(h_i)$, is investigated. The partial probabilities p, q, r take on values within the interval $[0, 1]$ consistent with the constraint $p + q + r = 1$, asymmetric distribution, h_i is the random field variable with basic absolute value h_0 (strength); λ is the competition parameter, which is the ratio between the respective strength of the random magnetic field in the two principal directions ($+z$) and ($-z$) and is positive so that the random fields are competing, anisotropic distribution. This probability distribution is an extension of the bimodal one allowing for the existence in the lattice of non magnetic particles or vacant sites. The current random field Ising system displays mainly second order phase transitions, which, for some values of p, q and h_0 , are followed by first order phase transitions joined smoothly by a tricritical point; occasionally, two tricritical points appear implying another second order phase transition. In addition to these points, re-entrant phenomena can be seen for appropriate ranges of the temperature and random field for specific values of λ, p and q . Using the variational principle, we write down the equilibrium equation for the magnetization and solve it for both phase transitions and at the tricritical point in order to determine the magnetization profile with respect to h_0 , considered as an independent variable in addition to the temperature.

Key words: Ising model, asymmetric bimodal random field, anisotropic interactions, phase-diagram, tricritical point, phase transitions

PACS: 05.50.+q, 75.10.Hk, 75.10.Nr, 64.60.Kw

* Corresponding author.

Email address: ihatziag@phys.uoa.gr (Ioannis A. Hadjiagapiou).

1 Introduction

Prediction of the critical behavior of modified spin models (site or bond diluted, random bonds, random fields), called disordered systems, has been the subject of many studies in the last decades, since this modification brings about considerable changes in the critical behavior of these systems, such as replacement of a first-order phase transition (FOPT) by a second-order phase transition (SOPT), depression of tricritical points and critical end points, new critical points and universality classes, etc [1,2,3]. The study of the disordered systems is based on the standard models, Ising, Blume-Capel, Baxter-Wu, Heisenberg, etc, modified accordingly to meet the case under consideration. Furthermore, extensions and versions of these models can be applied to describe many other different situations, such as multicomponent fluids, ternary alloys, ^3He - ^4He mixtures, in addition to the magnetic systems for which these were initially conceived. The most extensively studied model in statistical and condensed matter physics is the spin-1/2 Ising model, since its two dimensional version was analytically solved by Onsager (without an external magnetic field); as a consequence, it has formed the prototype for various generalizations. In its modified versions, it exhibits a variety of multicritical phenomena, such as a phase diagram with ordered ferromagnetic and disordered paramagnetic phases separated by a transition line that changes from an SOPT to an FOPT joined by a tricritical point (TCP); besides these, critical points, critical end points, ordered critical points of various orders, re-entrance can appear as in the presence of random fields. The multicritical phenomena appear in systems presenting competition among distinct types of ordering and there are numerous circumstances in which this kind of phenomenon can arise. In ferromagnetic systems in the presence of random fields, the competition is between the parallel and random orderings, causing, occasionally, the conversion of a continuous transition into an FOPT and the subsequent appearance of TCP as well as re-entrance in some cases. Random-field effects on magnetic systems have been systematically studied not only for their own merit but for their experimental importance, as well.

In two dimensions an infinitesimal amount of field randomness destroys any FOPT [3]. One such situation is the presence of random magnetic fields acting on each spin in an otherwise free of defects lattice; the respective pure system is considered to be described by Ising model, which is now transformed into the random field Ising model (RFIM) [4,5,6]. RFIM had been the standard vehicle for studying the effects of quenched randomness on phase diagrams and critical properties of lattice spin systems and was studied for many years since the seminal work of Imry and Ma [6]. Associated with this model are the notions of lower critical dimension, tricritical points, higher order critical points and random field probability distribution function (PDF). The simplest model exhibiting a tricritical phase diagram in the absence of randomness is the Blume-

Capel model – a regular Ising spin-1 model [7,8,9,10]. Although much effort has been invested in the study of the RFIM, the only well-established conclusion is the existence of a phase transition for $d \geq 3$ (d space dimension), that is, the critical lower dimension d_l is 2, resulted after a long controversial discussion [6,11], while many other questions are still unanswered; among them are those of the order of the phase transition, the existence of a tricritical point (TCP) and the dependence of these on the form of the random field PDF. According to the mean field approximation (MFA), the choice of the random field PDF can lead to a continuous ferromagnetic/paramagnetic (FM/PM) boundary as in the single Gaussian PDF, whereas for the symmetric bimodal PDF this boundary is divided into two parts, an SOPT branch for high temperatures and an FOPT branch for low temperatures separated by a TCP at $kT_c^t/(zJ) = 2/3$ and $h_c^t/(zJ) = (kT_c^t/(zJ)) \times \arg \tanh(1/\sqrt{3}) \simeq 0.439$ [12,13,14], where z is the coordination number, k is the Boltzmann constant and T_c^t, h_c^t are the tricritical temperature and random field, respectively, so that for $T < T_c^t$ and $h > h_c^t$ the transition to the FM phase is of first order. However, this behaviour is not fully elucidated since in the case of the three dimensional RFIM the high temperature series expansions yield only continuous transitions for both PDFs [15]; according to Houghton et al [16] both distributions (single Gaussian and bimodal) predict a tricritical point with $h_c^t = 0.28 \pm 0.01$ and $T_c^t = 0.49 \pm 0.03$ for the bimodal and $\sigma_c^t = 0.36 \pm 0.01$ and $T_c^t = 0.36 \pm 0.04$ for the Gaussian with critical standard deviation σ_c^t . Galam and Birman studied the crucial issue for the existence of a TCP within the mean field theory for a general PDF $p(\vec{H})$ (\vec{H} random magnetic field) by using an even degree free energy expansion up to eighth degree in the order parameter; they proposed some inequalities between the derivatives of the PDF up to sixth order at zero magnetic field for the possible existence of a TCP [17]. In Monte Carlo studies for $d = 3$, Machta et al [18], using a Gaussian distribution, could not reach a definite conclusion concerning the nature of the transition, since for some realizations of randomness the magnetization histogram was two-peaked (implying an SOPT) whereas for other ones it was three-peaked implying an FOPT; Middleton and Fisher [19], using a similar distribution for $T = 0$, suggested an SOPT with a small order parameter exponent $\beta = 0.017(5)$; Fytas et al [20], following the Wang-Landau and Lee entropic sampling schemes for the bimodal distribution function with random field strengths $h_0 = 2$ and $h_0 = 2.25$ for a simple cubic lattice found only an SOPT by applying the Lee-Kosterlitz free energy barrier method. Hernández and co-workers claim that they have found a crossover between an SOPT and an FOPT at a finite temperature and magnetic field for the bimodal distribution function [21]. One of the main issues was the experimental realization of random fields. Fishman and Aharony [22] have shown that the randomly quenched exchange interaction Ising antiferromagnet in a uniform field H is equivalent to a ferromagnet in a random field with the strength of the random field linearly proportional to the induced magnetization. Also another interesting result found by Galam [23] via the MFA was that the Ising anti-

ferromagnets in a uniform field with either a general random site exchange or site dilution have the same multicritical space as the random field Ising model with the bimodal PDF.

The usual PDF for the random field is either the symmetric bimodal

$$P(h_i) = p\delta(h_i - h_0) + q\delta(h_i + h_0) \quad (1)$$

where p is the fraction of lattice sites having a magnetic field h_0 , while the rest fraction $q = 1 - p$ of lattice sites has a field $(-h_0)$ and $p = q = \frac{1}{2}$ [12,24,25], or the Gaussian, single or double symmetric,

$$P(h_i) = \frac{1}{(2\pi\sigma^2)^{1/2}} \exp\left[-\frac{h_i^2}{2\sigma^2}\right]$$

$$P(h_i) = \frac{1}{2} \frac{1}{(2\pi\sigma^2)^{1/2}} \left\{ \exp\left[-\frac{(h_i - h_0)^2}{2\sigma^2}\right] + \exp\left[-\frac{(h_i + h_0)^2}{2\sigma^2}\right] \right\} \quad (2)$$

with mean value zero and $(h_0, -h_0)$, respectively, and standard deviation σ [13,26].

Galam and Aharony, in a series of investigations, presented a detailed analysis via the mean field and renormalization group of a system consisting of n -component classical spins (finally choosing $n = 3$) on a d -dimensional lattice of a uniaxially anisotropic ferromagnet in a longitudinal random field extracted from a symmetric bimodal PDF ($p = q = 1/2$) without and with a uniform magnetic field along the easy axis, respectively [27,28]. The uniaxial anisotropy was chosen to be along the easy axis and the exchange couplings were of the form $J^{(2)} = aJ^{(1)}$, where a is the anisotropy and $0 \leq a \leq 1$. Depending on the anisotropy (small, medium, large) a variety of phases (longitudinal, transverse, paramagnetic), critical points, bicritical points, and critical end points as well as a multicritical point (an intersection of bicritical, tricritical and critical-end-point lines) resulted. In addition to these purely theoretical investigations, Galam proposed a model (diluted random field) in his attempt to reproduce some of the features in the phase diagram of the experimental sample consisting of the mixed cyanide crystals $X(CN)_xY_{1-x}$, where X stands for an alkali metal (K,Na,Rb) and Y a spherical halogen ion (Br,Cl,I); the dilution of the pure crystal XCN is achieved by replacing CN by the halogen ions Y [29]. The pure alkali-cyanide XCN crystal ferroelastic transition disappears at some concentration x_c of the cyanide; its numerical value depends on both components X, Y . By choosing a model Hamiltonian (ferromagnetic Ising-type with nearest neighbor interaction) with dilution and a symmetric trimodal PDF for the random fields Galam, using MFA, managed to predict the involved first and second order phase transitions with the interfering TCP

as well as the respective concentration for a phase transition to occur depending on the procedure considered. The random fields were necessary because there were experimental evidences that below x_c cyanide displayed orientational freezing and the random fields were used for fixing this orientation. The involved probability p_t in PDF as well as the critical threshold x_c were expressed in terms of microscopic quantities.

Recently, the asymmetric bimodal PDF (1) with $p \neq q$, in general, has also been studied in detail [30] as well as the respective one with random anisotropic interactions $P(h_i) = p\delta(h_i - h_0) + q\delta(h_i + \lambda * h_0)$ [31], with the competition parameter λ varying in the interval $[0, 1]$. The former study has revealed that for some values of p and h_0 , the PM/FM boundary is exclusively of second order; however, for some other ranges of these variables this boundary consists of two branches, a second order one and another of first order with an intervening TCP, thus confirming the existence of such a point, whose temperature depends only on the probability p in (1). In addition to these findings, re-entrance has occurred as well as complex magnetization profiles with respect the random field strength h_0 . For $p = q = 1/2$, the symmetric bimodal PDF, the results found by Aharony were confirmed [12]. In the latter study, the anisotropic interactions (introduced through the parameter λ , with $\lambda \in [0, 1]$) do not change the numerical value of the tricritical temperatures (they still depend on p only), whereas the TCP random field (h_0^{TCP}) as well as auxiliary one (V_0^{TCP}) change as λ varies. Another important influence of λ is to reduce the FM region allocated to the system as λ tends to 1 ($\lambda \rightarrow 1$) and simultaneously broaden the PM region; however, the overall structure of the phase diagram as a function of λ for a specific value of p is unchanged, the only influence of λ on it is to cause a parallel translation of the wider phase diagram, occurring for $\lambda = 0$ inwards, towards the T axis as λ increases, thus reducing the FM region; the largest reduction occurs for $\lambda = 1$.

An immediate generalization of the asymmetric bimodal (1) is the asymmetric trimodal one,

$$P(h_i) = p\delta(h_i - h_0) + q\delta(h_i + h_0) + r\delta(h_i) \quad (3)$$

where $p + q + r = 1$. In earlier studies, the partial probabilities p, q had been considered as equal and related to r by the relation $p = q = (1 - r)/2$, symmetric PDF [32,33]; recently unequal p, q , ($p \neq q$) were considered, asymmetric PDF [34]. The third-peak, introduced in addition to the other two ones in the bimodal (1) and associated with the third term in (3), is to allow for the presence of non magnetic particles or vacancies in the lattice that are not affected by the random magnetic fields and results in reducing the randomness of the system, as well. A direct result of the choice of this PDF is that the respective physical system, depending on the values of p, q, h_0 , can have one tricritical point and, in some cases, it can have two such points, in

contrast to the bimodal PDF, which has only one such point in both versions, [30,31].

For the critical exponents of the three-dimensional RFIM, it seems that there is broad consensus concerning their values except for the specific heat exponent α , for which there is much dispute concerning its numerical value, since its sign is widely accepted to be negative. The main sources of information for the critical exponents are Monte Carlo simulations. However, they provide various values depending on the probability distribution considered. Middleton and Fisher concluded that the α -exponent is near zero, $\alpha = -0.01 \pm 0.09$ [19]. Rieger and Young, considering the bimodal distribution, estimated $\alpha = -1.0 \pm 0.3$ [35], Rieger, using the single Gaussian distribution, estimated $\alpha = -0.5 \pm 0.2$ [36], whereas Hartmann and Young, from ground-state calculations, estimated $\alpha = -0.63 \pm 0.07$ [37]. Nowak et al estimated that $\alpha = -0.5 \pm 0.2$ [38], whereas Dukovski and Machta found a positive value, namely, $\alpha = 0.12$ [39]. Malakis and Fytas [40], by applying the critical minimum-energy subspace scheme in conjunction with the Wang-Landau and broad-histogram methods for cubic lattices, proved that the specific heat and susceptibility are non-self-averaging using the bimodal distribution. The same ambiguous situation prevails in experimental measurements; see Ref. [41].

Another possible generalization for the trimodal PDF (3) is to assume that the random field takes on different values in the up and down directions (anisotropy), namely,

$$P(h_i) = p\delta(h_i - h_0) + q\delta(h_i + \lambda * h_0) + r\delta(h_i) \quad (4)$$

where λ (competition parameter) is the ratio of the two fields in the up and down directions with $\lambda \in [0, 1]$, since for $\lambda < 0$ the two random fields will act in the same direction without competition, see also Ref. [31].

In this work, we study the RFIM with the asymmetric and anisotropic trimodal PDF (4) with arbitrary values for the partial probabilities p, q and λ in order to investigate the phase diagrams, phase transitions, tricritical points and magnetization profiles with respect to h_0 and compare these results with those of the isotropic case ($\lambda = 1$) studied earlier [34]. The paper is organized as follows. In the next section, the suitable Hamiltonian is introduced, and the respective free energy and equation of state for the magnetization are derived. In section 3, the phase diagram, tricritical points and magnetization profiles for various values of λ and p, q are calculated and discussed; we close with the conclusions in section 4.

2 The model

The Ising model Hamiltonian in the presence of random fields is written as

$$H = -J \sum_{\langle i,j \rangle} S_i S_j - \sum_i h_i S_i, \quad S_i = \pm 1. \quad (5)$$

The summation in the first term extends over all nearest neighbors and is denoted by $\langle i, j \rangle$; in the second term h_i represents the random field that couples to the one-dimensional spin variable S_i . We also consider that $J > 0$ so that the ground state is ferromagnetic in the absence of random fields. The presence of randomness involves two averaging procedures, the usual thermal average, denoted by angular brackets $\langle \dots \rangle$, and the disorder average over the random fields denoted by $\langle \dots \rangle_h$ for the respective PDF.

For the asymmetric ($p \neq q$) and anisotropic ($\lambda \neq 1$) bimodal/trimodal PDFs, we also make additional assumptions concerning the random field moments

$$\langle h_i \rangle_h = (p - \lambda q)h_0, \quad \langle h_i h_j \rangle_h = h_0^2 \delta_{ij} \quad (6)$$

The former relation in (6) vanishes for a symmetric and isotropic PDF ($p = q, \lambda = 1$), whereas for an asymmetric PDF ($p \neq q$) is non-zero implying that the system is under the influence of a residual magnetic field due to the asymmetry and anisotropy of the random field, thereby affecting system's magnetization; a similar case has appeared in Ref. [30,31,34], as well. The latter relation implies that there is no correlation between h_i at different lattice sites.

According to the MFA the Hamiltonian (5) takes the form [12,13,25,30,31,34]

$$H_{MFA} = \frac{1}{2} N z J M^2 - \sum_i (z J M + h_i) S_i \quad (7)$$

where N is the number of spins and M the magnetization; the respective free energy per spin within the MFA is

$$\begin{aligned} \frac{1}{N} \langle F \rangle_h &= \frac{1}{2} z J M^2 - \frac{1}{\beta} \langle \ln \{ 2 \cosh[\beta(z J M + h_i)] \} \rangle_h \\ &= \frac{1}{2} z J M^2 - \frac{1}{\beta} \int P(h_i) \ln \{ 2 \cosh[\beta(z J M + h_i)] \} dh_i \end{aligned} \quad (8)$$

where the probability $P(h_i)$ is chosen to be the modified trimodal (4), $\beta = 1/(kT)$, T is the temperature.

The magnetization is the solution to the Eq. $d(\langle F \rangle_h / N) / dM = 0$ (equilibrium condition)

$$M = \langle \tanh[\beta(zJM + h_i)] \rangle_h \quad (9)$$

If the distribution $P(h_i)$ under consideration is symmetric, $P(h_i) = P(-h_i)$, which occurs for $p = q = (1 - r)/2$ and $\lambda = 1$, then the case $M = 0$ (PM phase) will always be a solution to (9); otherwise this shall not be the case. However, this can be remedied if an auxiliary field V_0 is introduced into the system such that [12,30,31,34]

$$\langle \tanh[\beta(h_i + V_0)] \rangle_h = 0, \quad (10)$$

inducing the PM phase; the solution to this equation is V_0 for specific values of h_i and β . However, this relation acts as a constraint on the system influencing, nevertheless, its behaviour. The free energy (8) in the presence of the auxiliary field V_0 takes, now, the form

$$\begin{aligned} \frac{1}{N} \langle F \rangle_h &= \frac{1}{2} zJM^2 - \frac{1}{\beta} \langle \ln \{ 2 \cosh[\beta(zJM + h_i + V_0)] \} \rangle_h \\ &= \frac{1}{2} zJM^2 - \frac{1}{\beta} \left\{ F_0 + \frac{\alpha^2 F_2}{2!} M^2 + \frac{\alpha^3 F_3}{3!} M^3 + \frac{\alpha^4 F_4}{4!} M^4 + \right. \\ &\quad \left. \frac{\alpha^6 F_6}{6!} M^6 \right\} \end{aligned} \quad (11)$$

after expanding the quantity in angular brackets in powers of M and calculating the average values using (4) with $\alpha \equiv \beta Jz$. By setting $t_i \equiv \tanh[\beta(V_0 + h_i)]$, $t_+ \equiv \tanh[\beta(V_0 + h_0)]$, $t_- \equiv \tanh[\beta(V_0 - \lambda * h_0)]$ and $t_0 \equiv \tanh[\beta V_0]$ we get

$$\begin{aligned} F_0 &= \langle \ln \{ 2 \cosh[\beta(V_0 + h_i)] \} \rangle_h \\ &= \ln 2 + p \ln \cosh[\beta(V_0 + h_0)] + q \ln \cosh[\beta(V_0 - \lambda * h_0)] + r \ln \cosh[\beta V_0] \\ F_1 &= \langle t_i \rangle_h = pt_+ + qt_- + rt_0 \\ F_2 &= \langle 1 - t_i^2 \rangle_h = 1 - pt_+^2 - qt_-^2 - rt_0^2 \\ F_3 &= \langle -2t_i(1 - t_i^2) \rangle_h \\ &= -2pt_+(1 - t_+^2) - 2qt_-(1 - t_-^2) - 2rt_0(1 - t_0^2) \\ F_4 &= \langle 2(1 - t_i^2)(3t_i^2 - 1) \rangle_h \\ &= 2p(1 - t_+^2)(3t_+^2 - 1) + 2q(1 - t_-^2)(3t_-^2 - 1) + 2r(1 - t_0^2)(3t_0^2 - 1) \\ F_6 &= \langle 8(1 - t_i^2)(15t_i^4 - 15t_i^2 + 2) \rangle_h \\ &= 8p(1 - t_+^2)(15t_+^4 - 15t_+^2 + 2) + 8q(1 - t_-^2)(15t_-^4 - 15t_-^2 + 2) \\ &\quad + 8r(1 - t_0^2)(15t_0^4 - 15t_0^2 + 2) \end{aligned} \quad (12)$$

The condition (10), for the existence of the PM phase for any value of p, q, λ , is equivalent to $F_1 = 0$,

$$pt_+ + qt_- + rt_0 = 0 \quad (13)$$

The equilibrium magnetization is a solution to the condition $d(\langle F \rangle_h / N) / dM = 0$, equivalent to

$$M = \alpha F_2 M + \frac{\alpha^2 F_3}{2!} M^2 + \frac{\alpha^3 F_4}{3!} M^3 + \frac{\alpha^5 F_6}{5!} M^5 \quad (14)$$

or

$$M = AM + BM^2 + CM^3 + EM^5 \quad (15)$$

$$A \equiv \alpha F_2, B \equiv \frac{\alpha^2 F_3}{2!}, C \equiv \frac{\alpha^3 F_4}{3!}, E \equiv \frac{\alpha^5 F_6}{5!} \quad (16)$$

In RFIM if there is a phase transition it will be associated with the magnetization and the involved two phases are the PM with $M = 0$ and the FM with $M \neq 0$. The resulting phase boundary is found by solving Eq. (15) in conjunction with the free energy (11) and condition (13). The SOPT boundary is determined by setting $A = 1$ and $C < 0$, whereas the FOPT boundary is determined by $A = 1$ and $C > 0$. These two boundaries, whenever they appear sequentially for the same values of the parameters λ, p, q , are joined at a tricritical point determined by the condition $A = 1$ and $C = 0$ [12,13,16,24,25,30,34,42], provided that $E < 0$ (equivalently, $F_6 < 0$) for stability [30,34,43,44]. However, for the FOPT boundary we shall also use the equality of the respective free energies $F(M = 0) = F(M \neq 0)$, where $F \equiv \langle F \rangle_h / N$.

3 Phase diagram. Tricritical Point. Magnetization profiles

The TCP coordinates $(T^{TCP}, h_0^{TCP}, V_0^{TCP})$, according to the definition of this point in the previous paragraph, are solutions to the simultaneous equations

$$\begin{aligned} pt_+ + qt_- + rt_0 &= 0 \\ pt_+^2 + qt_-^2 + rt_0^2 + 1/\alpha &= 1 \\ 4(pt_+^2 + qt_-^2 + rt_0^2) - 3(pt_+^4 + qt_-^4 + rt_0^4) &= 1 \end{aligned} \quad (17)$$

which do not lead to analytical formulas for these coordinates for both forms of the trimodal PDF (anisotropic and isotropic); on the contrary, the bimodal

PDF (resulting from the trimodal by setting $r = 0$), even in the presence of anisotropy, leads to analytical formulas; namely, the respective tricritical temperature T^{TCP} satisfies the second-degree equation

$$3(Q - 1)\alpha_{TCP}^2 + 2(2 - 3Q)\alpha_{TCP} + 3Q = 0 \quad (18)$$

where $Q = (p^3 + q^3)/qp$, thus T^{TCP} is a function only of the probability p and independent of the competition parameter λ [30]. The relevant discriminant of Eq. (18) is real in the interval $(13 - \sqrt{13})/26 \cong 0.37... \leq p \leq (13 + \sqrt{13})/26 \cong 0.63...$, so only for these values of p there exist tricritical points and both phase transitions take place for the same p , but for different temperatures and h_0 s. The two solutions to Eq. (18) determine the respective tricritical temperatures (in units of (Jz/k)), the upper and lower ones

$$\frac{kT_{\pm}^{TCP}}{Jz} = \frac{3(Q - 1)}{3Q - 2 \pm (4 - 3Q)^{1/2}} \quad (19)$$

We retain only the minus solution T_-^{TCP} , since the plus one T_+^{TCP} does not lead to physical results and is thus neglected, see Ref. [30].

The remaining coordinates h_0^{TCP} and V_0^{TCP} for the bimodal PDF are

$$\begin{aligned} h_0^{TCP} &= \frac{1}{2(1 + \lambda)} \ln \left[\left(\frac{1 + z_2}{1 - z_2} \right) \left(\frac{1 + z_1}{1 - z_1} \right) \right] \frac{kT_-^{TCP}}{zJ} \\ V_0^{TCP} &= \frac{1}{2(1 + \lambda)} \ln \left[\left(\frac{1 + z_2}{1 - z_2} \right)^\lambda \left(\frac{1 - z_1}{1 + z_1} \right) \right] \frac{kT_-^{TCP}}{zJ} \end{aligned} \quad (20)$$

where $z_1 = \sqrt{p(\alpha_-^{TCP} - 1)/(q\alpha_-^{TCP})}$ and $z_2 = \sqrt{q(\alpha_-^{TCP} - 1)/(p\alpha_-^{TCP})}$; h_0^{TCP} and V_0^{TCP} depend on both parameters p and λ (unlike T_-^{TCP}) as well as on the tricritical temperature itself T_-^{TCP} .

In order to examine the validity of the process under consideration, we focus on the well-studied symmetric and isotropic bimodal PDF (1), resulting from (4) by setting $p = q = 1/2$, $r = 0$ and $\lambda = 1$ with respective $Q = 1$; the plus solution vanishes ($kT_+^{TCP}/(Jz) = 0$), whereas the minus solution ($kT_-^{TCP}/(Jz)$) is singular; however, this singularity can be removed either by using the de L'Hôpital rules in Eq. (19) or by setting in (18) $Q = 1$, so that ($kT_-^{TCP}/(Jz)$) equals $(2/3)$ in agreement with the tricritical temperature in Ref. [12], see also Refs. [30,31,34].

For the current model, the system of Eqs. (17) can be solved only numerically for determining the TCP coordinates; this is achieved only for a lim-

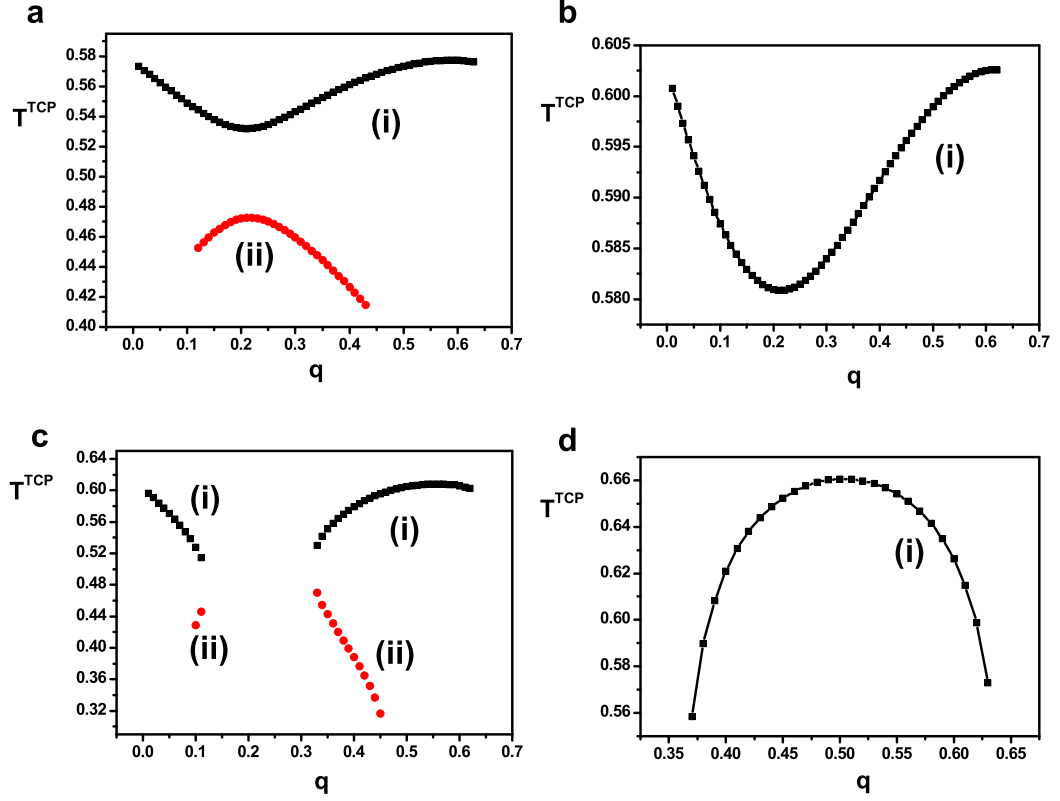


Fig. 1. (Color online) Representative graphs for the variation of the tricritical temperature for various values of the competition parameter λ and probability p against the probability q . The labels (i) (black symbols) and (ii) (red symbols) refer to the upper and lower TCP temperatures, respectively, in case two such temperatures exist for the same λ and p . Panels (a) and (b) correspond to $\lambda = 0.25$, for $p = 0.37$ and $p = 0.38$, respectively; panel (c) $\lambda = 0.50$ and $p = 0.38$; panel (d) $\lambda = 0.75$ and $p = 0.01$. T^{TCP} is in units of (Jz/k) .

ited number of p 's and q 's for specific λ values; for the TCP point, in general, $p \in [0.0, x]$, in this interval the numerical value of the upper bound x depends upon the specific λ value, but, in any case, it satisfies the inequality $x \leq (13 + \sqrt{13})/26 \cong 0.63\dots$; the respective q values depend on the specific p values, but they also lie in same interval as p . When p takes on the value $p = (13 - \sqrt{13})/26 \cong 0.37\dots$ (which is the lower bound of the probability p for the bimodal PDF to have tricritical points), then q takes on all the values within the interval $[0, (13 + \sqrt{13})/26 \cong 0.63\dots]$; for $(13 - \sqrt{13})/26 \leq p \leq (13 + \sqrt{13})/26$, the maximum possible value for q is such that $p + q = 1$ so that $r = 0$. The resulting tricritical temperatures exhibit a variety of variations as functions of the competition parameter λ and site probabilities p, q ; such graphs appear in Fig. 1. However, for some p and q values two tricritical temperatures occur, the upper ones (shown in black) and the lower ones (shown in red) as in Figs. 1(a,c) [45,46]. In panel (c) the TCP temperatures are grouped into two sets, the left-hand side one for small q 's and the right-hand side one for larger q 's; also, in this panel, the lack of points in the interval $[0.12, 0.32]$ of the q -axis is due to the absence of tricritical points in this interval, thus forming the existing gap; a similar behavior is also observed for another values of λ, p, q .

The variation of the random field values at the TCP, h_0^{TCP} , resulting from Eqs. (17) appears in Fig. 2, where various modes of variation are shown, displaying monotonic and non monotonic behavior. The gap in panel Fig. 2(c) is due to the absence of tricritical points for these values of λ, p, q as in Fig. 1(c). A similar picture appears for the auxiliary field at the tricritical point, V_0^{TCP} , but its variation is not so abrupt as that of h_0^{TCP} , see Fig. 3.

Another important quantity is the magnetization at the TCP. The equilibrium Eq. (14) at the tricritical point assumes the form,

$$\frac{\alpha^2 F_3}{2!} M^2 + \frac{\alpha^5 F_6}{5!} M^5 = 0 \quad (21)$$

or

$$F_6 \omega^5 + 60 F_3 \omega^2 = 0 \quad (22)$$

where $\omega \equiv \alpha M$ by taking into account the conditions for the TCP. The latter equation has the solutions,

$$\omega_1^{TCP} = 0 \quad (23)$$

$$\omega_2^{TCP} = \left(-60 F_3 / F_6 \right)^{1/3} \quad (24)$$

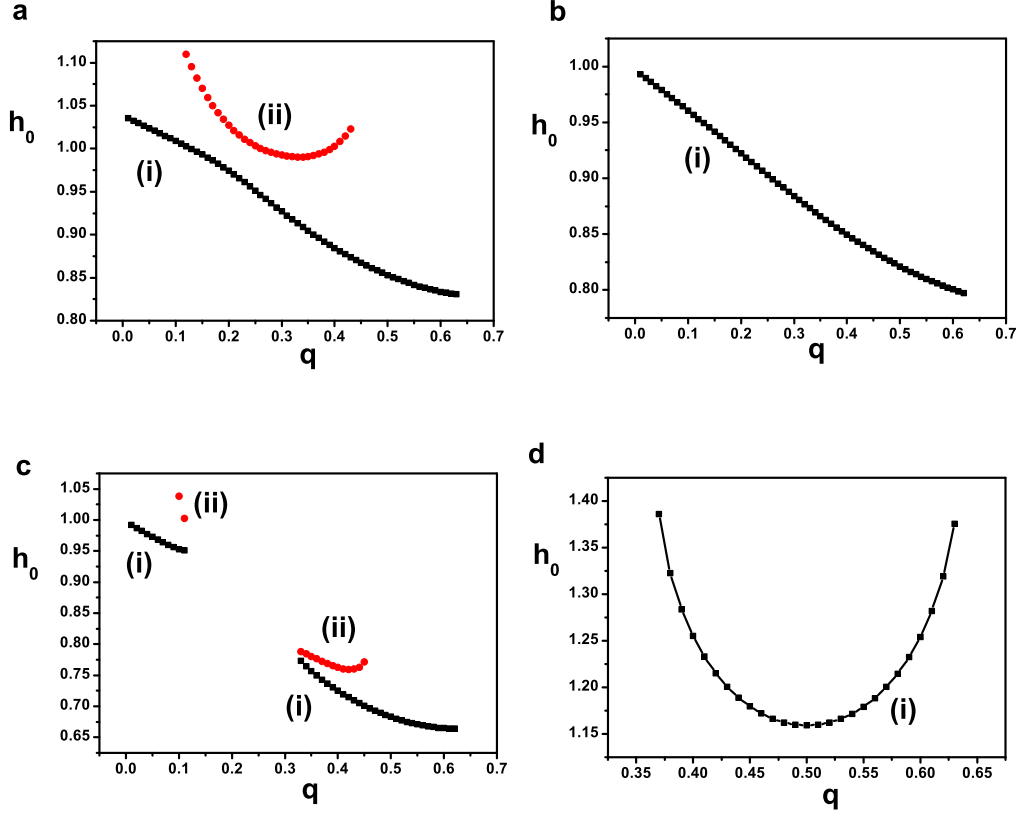


Fig. 2. (Color online) Indicative modes of variation for the random field strength h_0 with q for specific values of λ and p at the tricritical point; the labels (i) (black symbols) and (ii) (red symbols) refer to the quantities corresponding to the upper and lower TCP temperatures, respectively, in case two such temperatures exist. Panel (a) corresponds to $\lambda = 0.25, p = 0.37$; panel (b) $\lambda = 0.25, p = 0.38$; panel (c) $\lambda = 0.50, p = 0.38$; panel (d) $\lambda = 0.75, p = 0.01$. The random field h_0 exhibits monotonic and non-monotonic behavior with q . h_0 is in units of (Jz) , i.e., $h_0 \equiv h_0/(Jz)$.

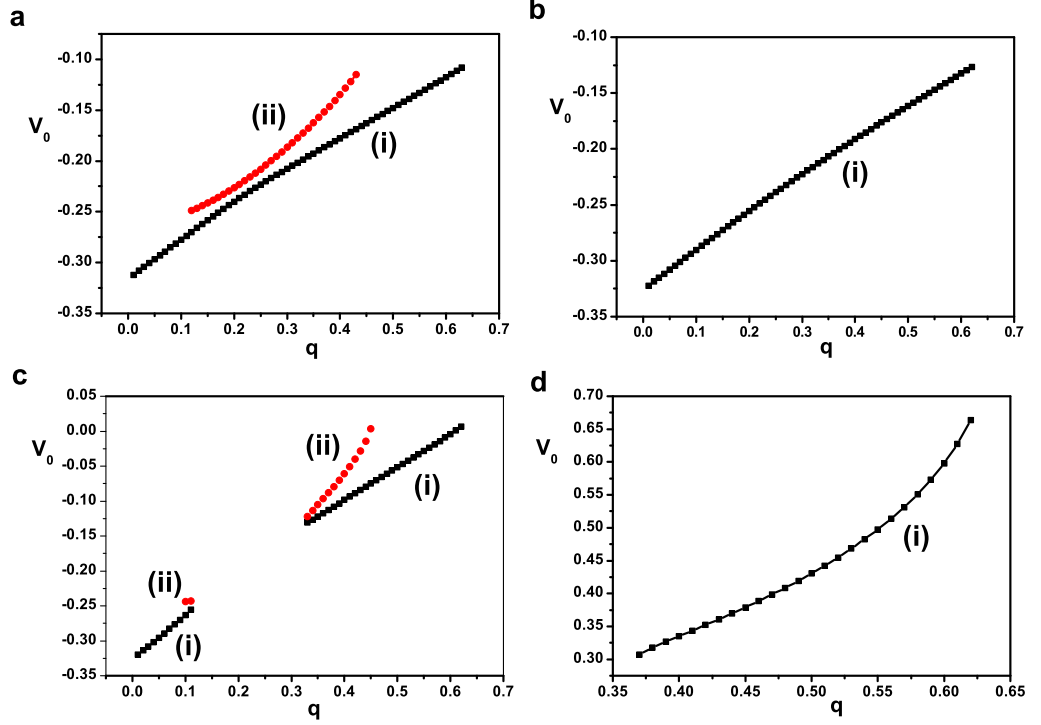


Fig. 3. (Color online) Modes of variation of the auxiliary field V_0 with q for specific values of λ and p at the tricritical point; the labels (i) (black symbols) and (ii) (red symbols) refer to the quantities corresponding to the upper and lower TCP temperatures, respectively, in case two such temperatures exist. Panel (a) corresponds to $\lambda = 0.25, p = 0.37$; panel (b) $\lambda = 0.25, p = 0.38$; panel (c) $\lambda = 0.50, p = 0.38$; panel (d) $\lambda = 0.75, p = 0.01$. The auxiliary potential V_0 exhibits monotonic behavior with q . V_0 is in units of (Jz) , i.e., $V_0 \equiv V_0/(Jz)$.

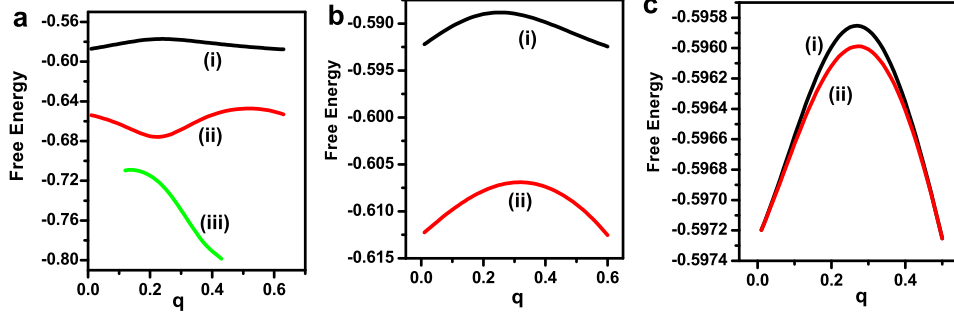


Fig. 4. (color online) Free energy of the zero (23) and non zero magnetization (24) at the tricritical point for $\lambda = 0.25$ and $p = 0.37$ (panel (a)), $p = 0.40$ (panel (b)) and $p = 0.50$ (panel (c)). In all panels, graph (i) corresponds to the zero solution M_1 and graphs (ii,iii) to the non zero solutions M_2 associated with the upper and lower TCP temperatures, respectively; the zero magnetization free energy (i) is higher than the one for the non zero magnetizations (ii,iii), implying that the non zero solution is the stable one.

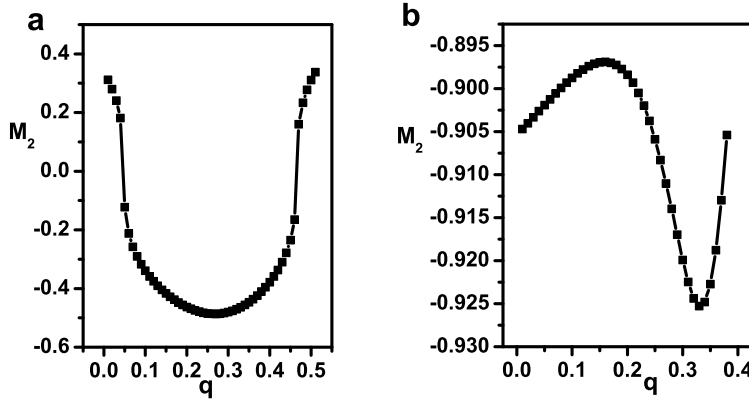


Fig. 5. The tricritical nonzero magnetization $M_2 = \left(-60F_3/F_6\right)^{1/3}$ with respect to q for $\lambda = 0.50$, $p = 0.49$ panel (a), and $p = 0.62$ panel (b).

from which the magnetizations $M_{1,2}^{TCP} = \omega_{1,2}^{TCP} * (kT^{TCP}/(Jz))$ can be deduced. The non zero TCP magnetization M_2^{TCP} (24) has a lower free energy than the zero solution (23), implying that this is the stable solution at the tricritical point, see Fig. 4 for the respective free energies for $\lambda = 0.25$. In case two tricritical points exist, then the free energy of the non zero magnetization corresponding to the lower TCP temperature is smaller than the respective one for the non zero magnetization corresponding to the upper TCP temperature for the same q values. The plot of the TCP magnetization M_2^{TCP} appears in Fig. 5, exhibiting significant variation; however, for the symmetric probability distribution, $p = q = 0.50$ and $\lambda = 1$, M_2^{TCP} becomes identical with the zero solution, so that the zero solution, now, is the only one and becomes stable for these p and q values; this is, also, a result of the elimination of the residual magnetic field implied by the first relation in (6).

The stability of the non zero magnetization over the zero one is a direct consequence of the existence of the residual magnetic field due to the first relation in equation (6), since for the general case $p \neq q$ the mean value of the random field is non zero, which is equivalent to the presence of an external magnetic field in the system so that the magnetization at the tricritical point scales as $M_t \equiv M(T = T^{TCP}) \sim h_{TCP}^{1/\delta_t}$, where h_{TCP} is the random magnetic field and the tricritical exponent $\delta_t = 5$ according to the Landau theory [30,34,47,48,49].

In a previous communication [30], the PDF of the RFIM was selected to be the asymmetric bimodal (1); this system displayed a symmetric behavior at the tricritical point with respect to the probability p ; especially, two distinct tricritical points with respective probabilities p_1 and p_2 such that $p_1 + p_2 = 1$ have identical tricritical temperatures and random fields, whereas the respective auxiliary fields and non zero magnetizations are absolutely equal. A similar symmetry is also observed in the present model with respect to the probabilities p and q for a specific λ value; if the probabilities (p_1, q_1) and (p_2, q_2) of the modified trimodal (4) are such that $p_1 + p_2 = 1$, then these two systems have the same TCP temperatures and random fields, whereas the respective nonzero magnetizations M_2^{TCP} are absolutely equal; the auxiliary fields V_0^{TCP} are absolutely equal in case $\lambda = 1$. Additionally, these cases have equal the respective free energies for the zero magnetization ($F(p_1, q_1, M_1^{TCP} = 0) = F(p_2, q_2, M_1^{TCP} = 0)$) as well as the nonzero ones ($F(p_1, q_1, M_2^{TCP}) = F(p_2, q_2, M_2^{TCP})$); the latter result implies that the two magnetizations $M_2^{TCP}(\lambda, p_1, q_1)$, $M_2^{TCP}(\lambda, p_2, q_2)$ are equally probable, an expected result, since the magnetizations have equal absolute values and the only difference being in their sign so that no direction is favored [34].

An important component in the study of magnetic or fluid systems is their phase diagram in which the general behavior of the system is shown; in the current case, it results as a solution to Eq. (15) by varying the parameters p, q, λ and appears in the Fig. 6 as $(h_0 - T)$ plots labelled by the individual λ value for specific p and q values. These plots are classified into two main groups: the first one includes those plots not possessing a TCP and corresponding only to an SOPT as in the Fig. 6(a) for $p = 0.35, q = 0.30$ for any λ value; the second group includes the plots possessing at least one TCP, which joins the FOPT branch with the SOPT branch of the phase diagram as in the Fig. 6(b, c, d) for $p = 0.40, q = 0.35, p = q = 0.50$ and $p = q = 0.45$, respectively. In the Fig. 6(b, d) the systems, described by the corresponding plots, have two TCPs (except the ones for $\lambda = 0.0$ Fig. 6(b,d) and $\lambda = 0.25$ Fig. 6(d)); the single and twin TCPs appear for another values of the parameters λ, p, q , as well. In some cases, a random system can present re-entrance that might be attributed to the competition between the exchange interaction (ordering factor) due to the first term in the Hamiltonian (5), on the one hand, and the random field (disorder factor), on the other hand, as in the Fig. 6(c, d); this effect is more pronounced in the Fig. 6(c). In re-entrance a vertical line in the (h_0, T) -plane

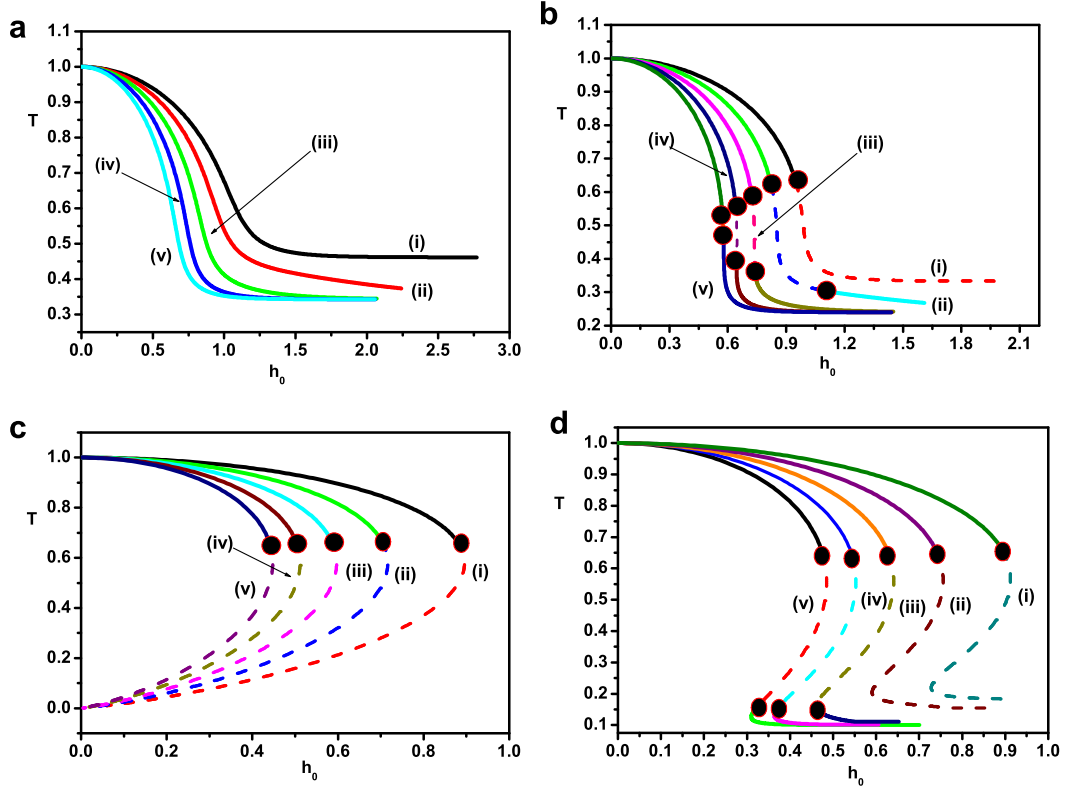


Fig. 6. (Color online) The phase boundaries for the PM/FM phase transitions for $\lambda = 0.00(i), 0.25(ii), 0.50(iii), 0.75(iv), 1.00(v)$, in all panels; $p = 0.35, q = 0.30$ (a), $p = 0.40, q = 0.35$ (b), $p = q = 0.50$ (c), $p = q = 0.45$ (d). A continuous line represents an SOPT and a dashed one an FOPT joined at a TCP, represented by a full circle. In panels (a, b) the system is in the FM phase for low temperatures and high h_0 s; on the contrary, in panel (c) it is in the PM phase for low temperatures due to re-entrance. In panel (c) the TCP temperatures are equal for any value of λ ($T^{TCP} = \frac{2}{3}$, see ref. [12]), whereas in panel (d) the upper TCP temperatures as well as the lower ones are not equal among themselves; the difference between the respective temperatures of two consecutive graphs is very small. Re-entrance is seen in panels (c, d). The temperature T is expressed in units of (Jz/k) , i.e., $T \equiv kT/(Jz)$.

crosses the transition line at least twice, in that, by lowering the temperature at constant h_0 , one observes firstly a *PM/FM* transition and then, on further lowering the temperature, an *FM/PM* transition appears, so the magnetization is zero although the temperature is low and the system remains in the PM phase for low temperatures as in the Fig. 6(c); occasionally, there can be another PM/FM transition (additional crossing) with the system returning to the FM phase for low temperatures and high h_0 s, Fig. 6(d). Re-entrance appears only in case an FOPT is present and its direct effect is to limit drastically the extent of the FM phase space as in the Fig. 6(c). However, within the MFA re-entrance may lead to nonphysical values (negative) for the spe-

cific heat, since energy will also present re-entrant behavior as magnetization because energy, within MFA, is proportional to the magnetization squared thus behaving similarly. The choice $\lambda = 0.00$ in the PDF (4) is a distinct case for this probability distribution, since the random magnetic field in the ($-z$) direction is eliminated and it refers to a lattice system in which some of its sites are either vacant or occupied by non-magnetic particles (site dilution, in this case the two last terms in (4) become similar and can be combined to a single term, $P(h_i) = p\delta(h_i - h_0) + (q + r)\delta(h_i)$), whereas the remaining sites are occupied by magnetic particles (fraction p) exposed to the random field whose direction is considered to be the positive z -direction without the presence of another competing random field; for this case the mean magnetization is expected to be higher than that for $\lambda \neq 0.00$ for the same p, q as long as there is not competition between random fields. In all panels of the Fig. 6 the respective phase boundary for $\lambda = 0.00$ is the outermost graph (i) with the widest FM phase region. However, as λ is switched on (at constant p, q) taking on values greater than zero, the random fields in the negative z direction appear and oppose the initially prevailing random fields (in the positive z direction), thus reducing the mean magnetization, causing the phase boundary to move towards to the temperature axis and, consequently, reducing the phase space allocated to the FM phase but simultaneously broadening the PM phase space; the former phase space attains its smallest extent for $\lambda = 1$, since the reduction is larger the higher the value of λ . The plots in the Fig. 6(a) correspond to systems in the FM phase for low temperatures and high random fields for any value of λ ; the critical temperatures seem to tend asymptotically to the limit $T_{cr} \cong 0.50$ for $\lambda = 0$ and $T_{cr} \cong 0.35$ for $\lambda \neq 0$, as $h_0 \rightarrow \infty$. In the Fig. 6(b) the critical temperatures tend asymptotically to the limit $T_{cr} \cong 0.35$ for $\lambda = 0$ and $T_{cr} \cong 0.25$ for $\lambda \neq 0$ as $h_0 \rightarrow \infty$; in the same limit in the Fig. 6(d) the critical temperatures tend asymptotically to the limit $T_{cr} \cong 0.1818\dots$ for $\lambda = 0$ and $T_{cr} \cong 0.1$ for $\lambda \neq 0$. The succession of phase transitions depends on the number of the tricritical points present although the SOPTs appear always for low fields and high temperatures: if there is only one TCP then the FOPTs appear for high fields and low temperatures; however, in case two TCPs are present the FOPTs appear for medium fields and temperatures, whereas the concluding phase transition is an SOPT for high fields and low temperatures. In the Fig. 6(b,d) the concluding phase transitions for those λ s with two TCPs are of second order and those with one TCP is of first order as well as in the Fig. 6(c). The aforementioned reduction of the FM-space due to the gradual increase of λ (control parameter) towards one ($\lambda \rightarrow 1$) has counterpart in the density profile of a spherical drop as a function of the inverse range parameter R of the strength of the attractive forces between the fluid particles; the overall structure of the density profile remains unchanged as a function of R in comparison to that with $R = 1$ except that the density profile either shrinks for $R > 1$ or widens for $R < 1$ to accommodate inside the drop the available particles [50]. A characteristic feature in panel (c), $p = q = 0.50$, is that the TCP temperatures, irrespective

of the λ -value, are all the same, namely $T^{TCP} = 2/3$; this value is identical to the one estimated by Aharony for the symmetric bimodal PDF [12].

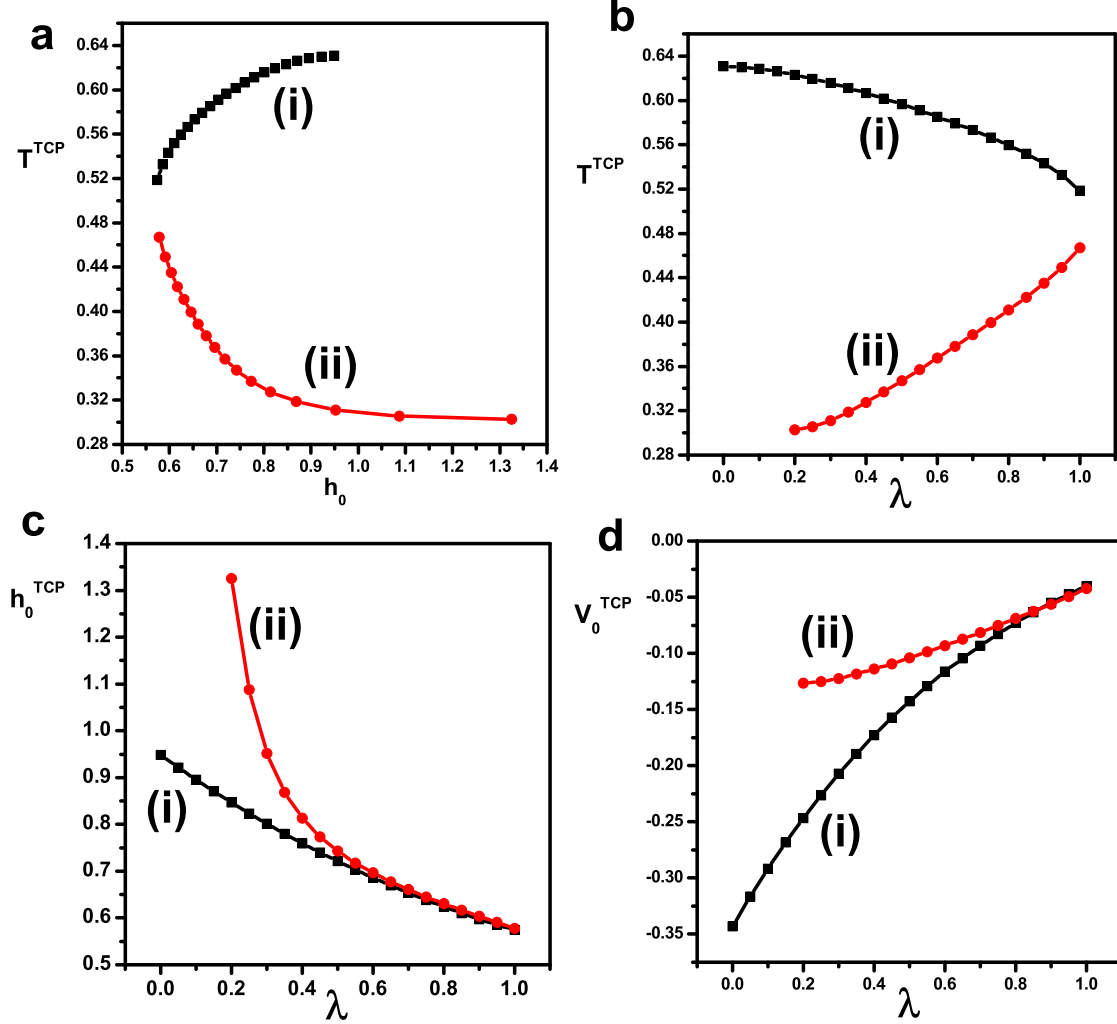


Fig. 7. (Color online) Tricritical point temperature T^{TCP} vs h_0 (panel (a)) as well as TCP coordinates (T, h_0, V_0) as functions of the competition ratio λ (panels (b,c,d)), for $p = 0.40, q = 0.35$; the labels (i) (black symbols) and (ii) (red symbols) refer to the quantities corresponding to the upper and lower TCP temperatures, respectively.

As it is evident from the Fig. 6(b), both groups of TCP temperatures regarded as functions of the TCP random field strength (h_0^{TCP}) display a systematic behavior, in that, they follow a decreasing route, which in the last stages (large h_0) becomes exponential as is revealed by the graphs in the Fig. 7(a) resulting by combining both groups of TCP temperatures. A similar system-

atic behavior is also followed by TCP temperature plotted with respect to the competition ratio λ , Fig. 7(b); the upper group of temperatures follow a decreasing route and the lower an increasing route tending to approach each other as λ tends to one, $\lambda \rightarrow 1$. Similarly, in Fig. 7(c) the random fields h_0^{TCP} as λ approaches 1, corresponding to the upper group of tricritical temperatures (*i*), decrease slowly, whereas those for the lower tricritical temperatures (*ii*) initially decrease abruptly but, in the last stages, decrease slowly tending to approach the ones of the upper temperatures. In addition, the TCP auxiliary fields V_0^{TCP} follow the inverse route in comparison to h_0^{TCP} : the V_0^{TCP} corresponding to the upper temperatures (*i*) follows a systematically increasing route, whereas those for the lower TCP temperatures (*ii*) are increasing very slowly, tending to approach the other group of V_0^{TCP} s as $\lambda \rightarrow 1$ Fig. 7(d).

An immediate connection of the Fig. 1 (describing the variation of the TCP temperature T^{TCP} with respect to p, q, λ) with the Fig. 6 (phase diagram) is the extent of the branches for the SOPTs and FOPTs with respect to these parameters. According to Fig. 1(b), T^{TCP} initially decreases implying that the respective SOPT branch increases at the expense of the FOPT branch acquiring its largest extent when the respective T^{TCP} has its minimum value for $\lambda = 0.25, p = 0.38, q = 0.21$, after this point the extent of the SOPT branch starts reducing and that for the FOPT increasing as the TCP temperature increases; the reverse behavior of the extent of the branches of SOPTs and FOPTs occurs for the case of Fig. 1(d) wherein the T^{TCP} initially increases. In case two such temperatures appear in the phase diagram, as in Fig. 1(a) and similar plots for other values of the aforementioned parameters, then the FOPT branch initially decreases acquiring its smallest extent when T^{TCP} becomes minimum in the upper branch and maximum in the lower branch, but later it starts increasing as the two temperatures get farther apart, whereas according to Fig. 1(c) in the respective phase diagram the extent of the FOPT branch continuously increases as the two TCP temperatures get farther apart with respect to q from the beginning for the right hand part; as far as the left hand one the SOPT branch, in general, increases.

Solving Eq. (15) to determine the phase diagram, the magnetization is also calculated for either phase transition. The condition $A = 1$ or $\alpha F_2(\beta, V_0, h_0) = 1$ leads to

$$pt_+^2 + qt_-^2 + rt_0^2 = \frac{\alpha - 1}{\alpha} \quad (25)$$

and by setting $T_2 \equiv pt_+^2 + qt_-^2 + rt_0^2$, (25) can be written

$$T_2 = \frac{\alpha - 1}{\alpha} \quad (26)$$

Inverting Eq. (26) the respective temperature for either phase transition can be determined, namely

$$\frac{kT}{Jz} = 1 - T_2 \quad (27)$$

In order to specify the type of the transition, the sign of $C \equiv \alpha^3 F_4/6$ is checked; however, to facilitate the calculations, the quantity C is rewritten as

$$C = \frac{\alpha^3}{3}[4T_2 - 3T_4 - 1] = \alpha^3[1 - T_4 - \frac{4}{3\alpha}] \quad (28)$$

using (26) and setting $T_4 = p t_+^4 + q t_-^4 + r t_0^4$. For an SOPT, C is negative [12], then (28) yields

$$T_4 > 1 - \frac{4}{3\alpha} \quad (29)$$

otherwise if

$$T_4 < 1 - \frac{4}{3\alpha} \quad (30)$$

the resulting transition is an FOPT. In order to determine the magnetization for an FOPT the expression (14) is combined with the equality of the respective free energies

$$F(M = 0) = F(M \neq 0) \quad (31)$$

or,

$$M^2 = F_2 \alpha M^2 + \frac{F_3}{3} \alpha^2 M^3 + \frac{F_4}{12} \alpha^3 M^4 + \frac{F_6}{360} \alpha^5 M^6 \quad (32)$$

Combining Eqs. (14), (32) and using the condition $\alpha F_2 = 1$, we get

$$F_6 \omega^3 + 10F_4 \omega = 0 \quad (33)$$

Eq. (33), is broken up into two equations; the first is $\omega_1 = 0$ or, equivalently, $M_1 = 0$ for the PM phase, whereas the other is

$$F_6 \omega^2 + 10F_4 = 0 \quad (34)$$

from which the nonzero solutions result, FM phase,

$$\omega_{2,3} = \pm \sqrt{-10F_4/F_6} \quad (35)$$

with $F_6 < 0$ as long as $F_4 > 0$ for an FOPT; the value for F_3 , consistent with (14) and (32), is $F_3 = -(F_4/6)\sqrt{-10F_4/F_6}$ for the positive root in (35) and $F_3 = (F_4/6)\sqrt{-10F_4/F_6}$ for the respective negative root. From the solution of this equation we can extract the magnetization $M = \omega * (kT/(Jz))$, since $\alpha = zJ/kT$ is already known from (27).

In plotting the phase diagram or the order parameter profile, the temperature is usually chosen as the independent variable; however, this is not the only choice as any other variable, suitably chosen, can be. In the present case the randomness strength h_0 is considered to be the control parameter for studying the variation of the non-zero positive magnetization $M_2 = \omega_2 * (kT/(Jz))$ for an FOPT, Eq. (35), by forming the respective magnetization profile as a function of h_0 for specific values of λ , p and q ; the negative solution $M_3 = -M_2$ behaves analogously. This study reveals a complicated structure for magnetization profiles and we present some representative of them; they appear in Fig. 8 displaying a variety of structures and characterized by critical points of several kinds. Apart from the simple profiles, with or without a critical point, there are also profiles forming closed loops (one or two), closed miscibility gap, Fig. 8. In addition to the usual critical points (indicated by the letter B in all graphs), there are double critical points (A points), critical end-points (C points) as well as double critical end-points (D points) [34,51]. This behavior can be considered as an FOPT between the two coexisting M_2 magnetizations with respect to randomness h_0 as long as this is now the control parameter, with upper and lower critical temperatures.

We consider, now, the values of p and q for which the system exhibits only an SOPT; Eq. (15) takes the form for $A = 1$,

$$F_6\omega^5 + 20F_4\omega^3 + 60F_3\omega^2 = 0 \quad (36)$$

The value $\omega_1 = 0$ is again a solution (two-fold) or, equivalently, $M_1 = 0$ (PM phase); the other three ones are the solutions to the equation

$$F_6\omega^3 + 20F_4\omega + 60F_3 = 0 \quad (37)$$

which, depending on the value of λ, p, q and h_0 , can have either only one real non zero solution if $\Delta = u^3 + v^2 \geq 0$ ($v = -30F_3/F_6$, $u = (20F_4)/(3F_6)$), namely

$$\omega_2 = \sqrt[3]{v + \sqrt{\Delta}} + \sqrt[3]{v - \sqrt{\Delta}} \quad (38)$$

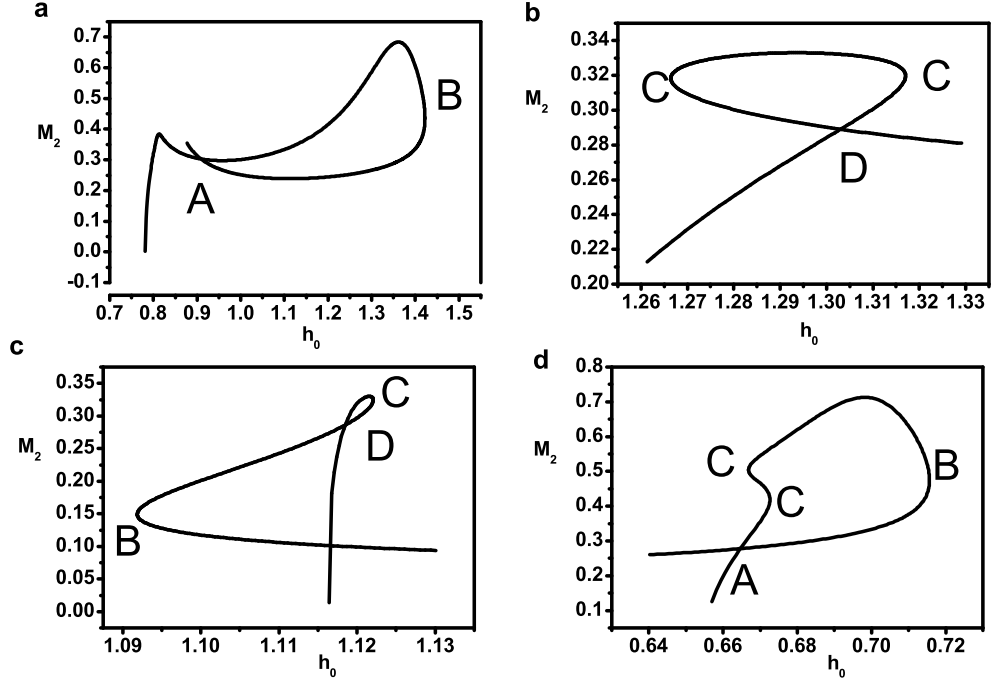


Fig. 8. Magnetization profile vs. h_0 for an FOPT. The first row corresponds to $\lambda = 0.25, p = 0.40, q = 0.50$ panel (a) and $\lambda = 0.50, p = 0.25, q = 0.55$ panel (b). The second row corresponds to $\lambda = 0.50, p = 0.30, q = 0.45$ panel (c) and $\lambda = 0.50, p = 0.40, q = 0.50$ panel (d). In all panels point A represents a double critical point, point B a regular critical point, point C a critical end-point, point D a double critical end-point.

or three real non zero solutions for $\Delta < 0$, which are

$$\begin{aligned}
 \omega_2 &= 2\sqrt[3]{\rho} \cos(\theta/3) \\
 \omega_3 &= -\sqrt[3]{\rho} [\cos(\theta/3) + \sqrt{3}\sin(\theta/3)] \\
 \omega_4 &= -\sqrt[3]{\rho} [\cos(\theta/3) - \sqrt{3}\sin(\theta/3)]
 \end{aligned} \tag{39}$$

where $\rho = \sqrt{v^2 - \Delta}$, $\theta = \arctan(\sqrt{-\Delta}/v)$ and $M_i = \omega_i * (kT/(Jz))$, $i = 2, 3, 4$. As a consequence, the solutions for an SOPT are classified into two groups, group 1 includes the zero-solution ($M_1 = 0$) and the single nonzero one M_2 of Eq. (38), whereas group 2 includes again the zero solution and the nonzero ones M_2, M_3, M_4 of the Eq. (39). Depending on the values of λ, p, q and h_0 , there can be transitions between these two groups. For the p values an FOPT is present, the solutions to the SOPT Eq. (37) belong to group 1; for small h_0 's the zero solution ($M_1 = 0$) is the stable, whereas for larger h_0 's (but smaller than those corresponding to the respective FOPT) the M_2 solution (38) is the stable.

The investigation was also extended to the zero-temperature case, $T = 0$; in this case the free energy (8) reduces to,

$$\begin{aligned}
F \equiv \frac{1}{N} \langle F \rangle_h &= \frac{1}{2} zJM^2 - \frac{1}{\beta} \langle \ln \{ 2 \cosh[\beta(zJM + h_i)] \} \rangle_h \\
&= \frac{1}{2} zJM^2 - \langle |zJM + h_i| \rangle_h \\
&= \frac{1}{2} zJM^2 - p|zJM + h_0| - q|zJM - \lambda * h_0| - r|zJM| \quad (40)
\end{aligned}$$

the external potential was omitted. Applying the equilibrium condition $dF/dM = 0$ to (40) we get,

$$M = p \frac{|zJM + h_0|}{zJM + h_0} + q \frac{|zJM - \lambda * h_0|}{zJM - \lambda * h_0} + r \frac{|zJM|}{zJM} \quad (41)$$

Analyzing Eq. (41), we find that $M = 1$ is a stable solution for $p+r > \lambda h_0/zJ$, whereas for $p+r < \lambda h_0/zJ$ the stable one is $M = 1 - 2q$. Also, across the boundary $\lambda h_0/zJ = p+r$ a first-order phase transition occurs between the two ordered phases with $M = 1$ and $M = 1 - 2q$. If we consider the symmetric trimodal PDF ($p = q = \frac{1-r}{2}, \lambda = 1$), the results found by Sebastianes and Saxena [33] are recovered, that is, the former result ($M = 1$) is stable for $\frac{1+r}{2} > h_0/zJ$, whereas the latter ($M = r$) for $\frac{1+r}{2} < h_0/zJ$, using the current notation. The physical explanation for the existence of the above two ordered phases is that they can be attributed to the competition between the ordering tendency, due to the first term in Eq. (5), and the disorder induced because of the presence of the second term in the same equation. In the first case, $M = 1$, the condition $(p+r) > (\lambda h_0/(zJ))$ implies that the exchange interaction J is much stronger than the randomness h_0 , and their ratio is always smaller than one, thus forcing the system's spins to order according to the first term in (5). The alternative condition $(p+r) < (\lambda h_0/(zJ))$ implies, now, that randomness is no longer negligible but strong enough to influence significantly the spins enforcing a p -fraction of them to point up and a q -fraction down, to randomly

align with the local fields, thus, practically, it dominates, so to speak, over the first term in Eq. (5) so that $M = p - q + r = 1 - 2q$. In addition to the aforementioned two solutions, there are more; the result $M = 2(p + q) - 1$ is stable for $p - r > \lambda h_0/zJ$, $M = 2p - 1$ for $p - r < \lambda h_0/zJ$, $M = 1 - 2p$ for $r - p > \lambda h_0/zJ$, $M = 1 - 2(p + q)$ for $r - p < \lambda h_0/zJ$ and $M = -1$ for $p + r + \lambda h_0/zJ > 0$.

4 Conclusions and discussions

In the current treatment we have determined the phase diagram and discussed some critical phenomena of the Ising model under the influence of a trimodal random field, an extension of the bimodal one to allow for the existence of non magnetic particles or vacancies in the system, for arbitrary values of the probabilities p and q and different strengths of the random field in the up and down directions specified by the competition parameter λ via the Landau expansion. The competition between the ordering effects and the randomness induces a rich phase diagram. The system is strongly influenced by the random field, which establishes a new competition favoring disorder; this is obvious from the appearance of first order transitions and tricritical points, in addition to the second order transitions for some values of λ, p and q ; the tricritical point temperature has various modes of variation as a function of p and q and for some cases there are two such points. The trimodal distribution induces re-entrant behavior for the appropriate range of p, q and random field h_0 . For some values of p and q the system can be found either in the PM phase or in the FM phase for low and medium temperatures and high random fields; a significant result is that the part of the phase diagram allocated to the FM phase is reduced significantly as λ tends to one. A direct consequence of the asymmetric and anisotropic PDF is the existence of residual mean magnetic field in the system, a result of $\langle h_i \rangle_h = (p - \lambda q)h_0$, making the TCP non zero magnetization M_2 to be the stable one in comparison to the zero one, M_1 . Both asymmetric PDFs, bimodal and trimodal, confirm the existence of a TCP and, nevertheless, yield similar magnetization profiles as well as re-entrance; however, the trimodal one predicts also the existence of a second TCP.

Griffiths extended the notion of the critical point to the so-called multicritical points, e.g., the tricritical point, the critical-end-point, double critical-end-point, fourth-order point, ordered critical point, etc. [52]; however, in order to describe these points (except the first two) the expansion considered for the free energy (11) has to be extended to higher-order terms [32,44,53,54] so that the stability criteria for such a point are satisfied, but this is beyond the scope of the current research.

The Landau theory breaks down close to the critical point (the non classical region) because as the transition temperature is approached the fluctuations

become important and non classical behavior is observed. A relative criterion, called the Ginzburg criterion, determines how closely to the transition temperature the true critical behavior is revealed, or, in other words, it governs the validity of the Landau theory close to a critical point [55]. This criterion can rely on any thermodynamic quantity but the specific heat is usually considered for determining the critical region around T_c where the mean field solution cannot correctly describe the phase transition. The Landau theory is valid for lattice dimensionality greater than the upper critical dimension $d_u = 4$ in the case of the presence of only thermal fluctuations. However, in the current case the presence of random fields enhances fluctuations causing the critical region to be wider than the one due only to the thermal fluctuations [56,57] and the upper critical dimension is increased by 2 to $d_u = 6$. Occasionally, the non classical region for some physical systems is extremely narrow so that the respective critical behavior expected from Landau theory is observed for a wide range of temperatures because, in this case, the fluctuation region is very narrow and hardly accessible for experimental observation; such a system is the weak-coupling superconductor in three dimensions for which the respective non classical region is $|t_{CR}| \leq 10^{-16}$ (t_{CR} is the reduced temperature, $t_{CR} = (T - T_c)/T_c$). However, on reducing the space dimension as in the case of the weak-coupling superconductor in two dimensions, the non classical region expands, so that the critical exponents have their classical values up to the interval $|t_{CR}| = 10^{-5}$, and thus the reduction of the space dimensionality has serious consequences for the critical behavior of the physical system; in contrast, there are systems with a wide non classical interval as in the case of the superfluid helium transition, for which the classical region extends up to $|t_{CR}| = 1.0$ and so fluctuations are detectable [58,59,60,61]. In addition to superconductivity, the extent of the non classical region for the ferroelectric system triglycine sulfate (TGS) is relatively small and its critical exponents have the respective classical values up to $|t_{CR}| = 1.5 \times 10^{-5}$ [62,63,64].

Our results indicate that on increasing the complexity of the model system new phenomena can be revealed as in the current case of including asymmetry in the PDF; this inclusion induces drastic changes in the phase diagram, such as re-entrance and two TCPs, thus confirming the necessity of treating the partial probabilities (p, q, r) of the PDF in the most general way to get the complete phase diagram. A similar situation appears in the model systems in Refs. [27,28] wherein the complexity considered has revealed a rich variety of phase diagrams with known and new multicritical points. The results obtained in the current investigation by using the MFA can provide a basis for a comprehensive analysis as well as experimental implementation. However, they are of no less importance, since they nevertheless show the phenomena that expected to be observed.

Acknowledgements

This research was supported by the Special Account for Research Grants of the University of Athens (*EΛKE*) under Grant No. 70/4/4096.

References

- [1] I. A. Hadjiagapiou, A. Malakis, S. S. Martinos, *Physica A* 387 (2008) 2256.
- [2] I. A. Hadjiagapiou I A, *Physica A* 390 (2011) 1279.
- [3] K. Hui, A. Nihat Berker, *Phys. Rev. Lett.* 62 (1989) 2507.
- [4] D. S. Fisher, G. M. Grinstein, A. Khurana, *Phys. Today* 41 (12) (1988) 56.
- [5] T. Nattermann, J. Villain, *Phase Transit.* 11 (1988) 5.
- [6] Y. Imry, S.-K. Ma, *Phys. Rev. Lett.* 35 (1975) 1399.
- [7] M. Blume, *Phys. Rev.* 141 (1966) 517.
- [8] H. W. Capel, *Physica* 32 (1966) 966.
- [9] A. Malakis, A. Nihat Berker, I. A. Hadjiagapiou, N. G. Fytas, *Phys. Rev. E* 79 (2009) 011125.
- [10] A. Malakis, A. Nihat Berker, I. A. Hadjiagapiou, N. G. Fytas, T. Papakonstantinou, *Phys. Rev. E* 81 (2010) 041113.
- [11] Imbrie J Z, *Phys. Rev. Lett.* 53 (1984) 1747.
- [12] A. Aharony, *Phys. Rev. B* 18 (1978) 3318.
- [13] T. Schneider, E. Pytte, *Phys. Rev. B* 15 (1977) 1519.
- [14] L. A. Fernández, A. Gordillo-Guerrero, V. Martín-Mayor, J. J. Ruiz-Lorenzo, *Phys. Rev. Lett.* 100 (2008) 057201.
- [15] M. Gofman, J. Adler, A. Aharony, A. B. Harris, M. Schwartz, *Phys. Rev. Lett.* 71 (1993) 2841; *Phys. Rev. B* 53 (1996) 6362.
- [16] A. Houghton, A. Khurana, F. J. Seco, *Phys. Rev. B* 34 (1986) 1700.
- [17] S. Galam, J. L. Birman, *Phys. Rev. B* 28 (1983) 5322.
- [18] J. Machta, M. E. J. Newman, L. B. Chayes, *Phys. Rev. E* 62 (2000) 8782.
- [19] A. A. Middleton, D. S. Fisher, *Phys. Rev. B* 65 (2002) 134411.
- [20] N. G. Fytas, A. Malakis, K. Eftaxias, *J. Stat. Mech.* (2008) P03015.
- [21] L. Hernández, H. T. Diep, *Phys. Rev. B* 55 (1997) 14080; L. Hernández, H. Ceva, *Physica A* 387 (2008) 2793.
- [22] S. Fishman, A. Aharony, *J. Phys. C: Solid State Phys.* 12 (1979) L729.
- [23] S. Galam, *Phys. Rev. B* 31 (1985) 7274.
- [24] M. Kaufman, M. Kanner, *Phys. Rev. B* 42 (1990) 2378.
- [25] D. Andelman, *Phys. Rev. B* 27 (1983) 3079.

- [26] N. Crokidakis, F. D. Nobre, *J. Phys.: Condens. Matter* 20 (2008) 145211.
- [27] S. Galam, A. Aharony, *J. Phys. C: Solid St. Phys.* 13 (1980) 1065.
- [28] S. Galam, *J. Phys. C: Solid St. Phys.* 15 (1982) 529.
- [29] S. Galam, *Europhys. Lett.* 37 (1997) 615; *J. of Non-Crystalline Solids* 235-237 (1998) 570.
- [30] I. A. Hadjiagapiou, *Physica A* 389 (2010) 3945.
- [31] I. A. Hadjiagapiou, *Physica A* 390 (2011) 3204.
- [32] M. Kaufman, P. Klunzinger, A. Khurana, *Phys. Rev. B* 34 (1986) 4766.
- [33] V. K. Saxena, *Phys. Rev. B* 35 (1987) 2055; R. M. Sebastianes, V. K. Saxena, *Phys. Rev. B* 35 (1987) 2058.
- [34] I. A. Hadjiagapiou, *Physica A* 390 (2011) 2229.
- [35] H. Rieger, A. Peter Young, *J. Phys. A: Math. Gen.* 26 (1993) 5279.
- [36] H. Rieger, *Phys. Rev. B* 52 (1995) 6659.
- [37] A. K. Hartmann, A. P. Young, *Phys. Rev. B* 64 (2001) 214419.
- [38] U. Nowak, K. D. Usadel, J. Esser, *Physica A* 250 (1998) 1.
- [39] I. Dukovski, J. Machta, *Phys. Rev. B* 67 (2003) 014413.
- [40] A. Malakis, N. G. Fytas, *Phys. Rev. E* 73 (2006) 016109; *Eur. Phys. J. B* 50 (2006) 39.
- [41] D. P. Belanger, A. P. Young, *J. Magn. Magn. Mater.* 100 (1991) 272.
- [42] A. Khurana, F. J. Seco, A. Houghton, *Phys. Rev. Lett.* 54 (1985) 357.
- [43] N. Crokidakis, F. D. Nobre, *Phys. Rev. E* 77 (2008) 041124.
- [44] O. R. Salmon, N. Crokidakis, F. D. Nobre, *J. Phys.: Condens. Matter* 21 (2009) 056005.
- [45] S. Galam, C. S. O. Yokoi, S. R. Salinas, *Phys. Rev. B* 57 (1998) 8370.
- [46] A. Weizenmann, M. Godoy, A. S. de Arruda, D. F. de Albuquerque, N. O. Moreno, *Physica B* 98 (2007) 297.
- [47] H. Eugene Stanley, *Introduction to Phase Transitions and Critical Phenomena*, Oxford, Clarendon Press, 1971.
- [48] H. S. Robertson, *Statistical Thermophysics*, New Jersey, Prentice-Hall, 1993, pp. 303, 308.
- [49] I. D. Lawrie, S. Sarbach, *Theory of Tricritical Points*, in *Phase Transitions and Critical Phenomena*, ed. C. Domb and J. L. Lebowitz, Academic Press, London, U.K., Vol. 9, 1984.

- [50] I. Hadjiagapiou, J. Phys.: Condens. Matter 7 (1995) 547.
- [51] I. Hadjiagapiou, R. Evans, Mol. Phys. 54 (1985) 383.
- [52] R. B. Griffiths, Phys. Rev. B 12 (1975) 345.
- [53] S. Galam, J. L. Birman, J. Phys. C : Solid State Phys. 16 (1983) L1145.
- [54] F. S. Milman, P. R. Hauser, W. Figueiredo, Phys. Rev. B 43 (1991) 13641.
- [55] V. L. Ginzburg, Fiz. Tverd. Tela. (Leningrad) 2 (1960) 2031 [Sov. Phys.-Solid State 2 (1961) 1824].
- [56] M. Kaufman, M. Kardar, Phys. Rev. B 31 (1985) 2913.
- [57] J. Als-Nielsen, R. J. Birgeneau, Amer. J. Phys. 45 (1977) 554.
- [58] A. Z. Patashinskii, V. I. Pokrovskii, Fluctuation Theory of Phase Transitions, Pergamon Press, Oxford, U.K., 1979.
- [59] Y. M. Ivanchenko, A. A. Lisyansky, Physics of Critical Fluctuations, Springer-Verlag, New York, U.S.A, 1995.
- [60] Domb C, The Critical Point: A Historical Introduction to the Modern Theory of Critical Phenomena, Taylor and Francis, London, U.K., 1996.
- [61] Goldenfeld N, Lectures On Phase Transitions And The Renormalization Group, Addison-Wesley, Reading, U.S.A., 1992.
- [62] K. Deguchi, E. Nakamura, Phys. Rev. B 5 (1972) 1072.
- [63] A. Mercado, J. A. Gonzalo, Phys. Rev. B 7 (1973) 3074.
- [64] T. Mitsui, E. Nakamura, M. Tokunaga, Ferroelectrics 5 (1973) 185; M. Tokunaga, T. Mitsui, Ferroelectrics 11 (1976) 451.